© 2022. Published by The Company of Biologists Ltd | Journal of Experimental Biology (2022) 225, jeb242929. doi:10.1242/jeb.242929

RESEARCH ARTICLE

Additive and epistatic effects influence spectral tuning in molluscan retinochrome opsin

G. Dalton Smedley[1], Kyle E. McElroy[1], Kathryn D. Feller[2] and Jeanne M. Serb[1,*]

ABSTRACT

The relationship between genotype and phenotype is non-trivial because of the often complex molecular pathways that make it difficult to unambiguously relate phenotypes to specific genotypes. Photopigments, comprising an opsin apoprotein bound to a light-absorbing chromophore, present an opportunity to directly relate the amino acid sequence to an absorbance peak phenotype (λ_{max}). We examined this relationship by conducting a series of site-directed mutagenesis experiments of retinochrome, a non-visual opsin, from two closely related species: the common bay scallop, *Argopecten irradians*, and the king scallop, *Pecten maximus*. Using protein folding models, we identified three amino acid sites of likely functional importance and expressed mutated retinochrome proteins *in vitro*. Our results show that the mutation of amino acids lining the opsin binding pocket is responsible for fine spectral tuning, or small changes in the λ_{max} of these light-sensitive proteins. Mutations resulted in a blue or red shift as predicted, but with dissimilar magnitudes. Shifts ranged from a 16 nm blue shift to a 12 nm red shift from the wild-type λ_{max}. These mutations do not show an additive effect, but rather suggest the presence of epistatic interactions. This work highlights the importance of binding pocket shape in the evolution of spectral tuning and builds on our ability to relate genotypic changes to phenotypes in an emerging model for opsin functional analysis.

KEY WORDS: Mutagenesis, Photopigment, Protein folding, Vision

INTRODUCTION

Understanding how genotype influences phenotype is a fundamental goal of biology. This relationship is far from trivial, as complex genetic pathways and environmental effects often preclude clear connections. The phototransduction system that converts light into electrical signals (Shichida and Matsuyama, 2009) offers a rare opportunity to examine genotype–phenotype relationships because single amino acid substitutions can drastically alter visual protein phenotype (Ueyama et al., 2002). Furthermore, because photopigments – the functional unit of phototransduction – only absorb a portion of the light spectrum, the wavelength of maximum absorbance (λ_{max}) represents a directly measurable phenotype.

Photopigments form by covalent bonds between a retinal chromophore and the binding pocket of an opsin apoprotein. The interactions of the chromophore with amino acids in the binding pocket have been highlighted as critical for photopigment function by theoretical calculations (Beppu and Kakitani, 1994; Beppu, 1997), mutagenesis (Nathans, 1990; Oprian et al., 1991; Yokoyama, 2000a,b; Van Hazel et al., 2013) and quantum mechanics/molecular mechanics (QM/MM) modeling (Melaccio et al., 2012; Ferré and Olivucci, 2003; González-Luque et al., 2000). Such interactions between the chromophore and the amino acid residues within the binding pocket of the opsin are thought to be responsible for modulating λ_{max}, or spectral tuning (Beppu and Kakitani, 1994; Irving et al., 1970). Changing amino acid side chains that affect the environment of the chromophore binding pocket may be particularly important (Lin et al., 1998).

Extensive mutagenesis efforts have been directed towards identifying spectral tuning sites in opsins (Merbs and Nathans, 1993; Hauser et al., 2014; Hunt et al., 2009; Hope et al., 1997). In vertebrates, λ_{max} differences between middle- and long-wavelength-sensitive pigments involved in color vision are attributed to three (Chan et al., 1992; Asenjo et al., 1994; Neitz et al., 1991) or five (Yokoyama and Radlwimmer, 1998, 1999) amino acid sites. These individual sites are responsible for small (nanometer) shifts that cumulatively alter the protein function (Yokoyama, 2000b). Whether the patterns of amino acid changes responsible for spectral tuning in vertebrate visual opsins are broadly applicable to the immense diversity of opsin proteins is unknown. This is because the vast majority of experimental spectral tuning research has been done in vertebrate visual systems (e.g. monostable G_t-protein-coupled opsins: reviewed in Hunt et al., 2007; Yokoyama, 2008), with a few exceptions in non-vertebrate species (e.g. bistable G_q-protein-coupled opsins: Wakakuwa et al., 2010; Saito et al., 2019; Terakita et al., 2008; Liénard et al., 2021; Frentiu et al., 2015; Nagata et al., 2019; and tetraopsins: Terakita et al., 2004, 2000). Moreover, the crystal structure of invertebrate opsins, such as G_q-protein-coupled opsins (e.g. squid and jumping spider 'rhodopsins'), has important differences compared with vertebrate opsins (G_t-protein-coupled opsins, e.g. bovine rhodopsin), such as greater organization in the cytoplasmic region correlating to bistability, an interconvertibility between the photopigment's dark state and its photoproduct (Varma et al., 2019; Shimamura et al., 2008; Murakami and Kouyama, 2008). This long-standing focus on vertebrate opsins has left us with a severe lack of understanding of how spectral tuning is controlled in invertebrate opsins.

To identify amino acids involved in the spectral tuning of photopigments, comparing the amino acid sequence and protein function of two closely related species is an effective starting point. Here, we cloned and expressed *in vitro* a mollusk-specific opsin, retinochrome, from two closely related scallops: the common bay scallop, *Argopecten irradians* (Lamarck 1819), and the king scallop, *Pecten maximus* (Linnaeus 1758). The two species have different ecologies: *A. irradians* is found in shallow (<10 m) protected estuarine waters among sea grass beds that trap suspended fine sediments (Clarke, 1965), while *P. maximus* occurs in deeper

[1]Department of Ecology, Evolution, and Organismal Biology, Iowa State University, Ames, IA 50011, USA. [2]Department of Biological Sciences, Union College, Schenectady, NY 12308, USA.

*Author for correspondence (serb@iastate.edu)

G.D.S., 0000-0001-7478-9225; K.E.M., 0000-0001-9581-2535; K.D.F., 0000-0003-4730-2105; J.M.S., 0000-0003-2112-470X

Received 26 May 2021; Accepted 26 April 2022

Journal of Experimental Biology (2022) 225, jeb242929. doi:10.1242/jeb.242929

(20–45 m) coastal waters with clean firm sand, fine gravel or sandy gravel bottoms (Duncan et al., 2016). Differences in depth, turbidity and substrate suggest different photic environments, which can influence spectral tuning of photopigments, such as retinochrome (Lythgoe et al., 1972).

Retinochrome is one of the few examples of a non-vertebrate, non-visual opsin with well-characterized biochemical and spectral properties (Hara and Hara, 1967, 1982, 1968; Hara et al., 1992, 1967; Ozaki et al., 1983). Further, its ease of expression and predictable nature in heterologous cell culture makes it a compelling protein to work with (Terakita et al., 2000). Retinochrome belongs to the 'photoisomerase' opsin clade of RGR/retinochrome/peropsin (Ramirez et al., 2016), and it is closely related to the mammalian retinal G-protein-coupled receptor (RGR) (Jiang et al., 1993) and the lepidopteran *unclassified opsin* (*UnRh*) and *RGR-like* genes (Macias-Muñoz et al., 2019) (Fig. 1). The protein is localized away from, but in close proximity to, the primary site of phototransduction; for example, the inner segments of retinal photoreceptor cells (Hara and Hara, 1982; Kingston et al., 2015) and pigment cell membranes of light-sensing chromatophores (Kingston et al., 2015) in cephalopods. Like other opsins, retinochrome possesses a lysine for, and a counterion that stabilizes, chromophore binding (Terakita et al., 2000). However, retinochrome does not mediate phototransduction like other opsins. Instead, it is a photoisomerase in the retinoid visual cycle of mollusks, converting all-*trans* retinal to 11-*cis* retinal following the absorption of light (Sperling and Hubbard, 1975). Whether a few amino acid substitutions cumulatively contribute to differences in retinochrome λ_{max} values, as seen in vertebrate visual opsins, is unknown.

We hypothesized that changing the shape (Hirayama et al., 1994) or electrostatic environment (Rinaldi et al., 2014) of retinochrome's binding pocket will shift the λ_{max} value. This shift would be the result of different biochemical properties of newly introduced amino acid residues, which can affect non-covalent interactions within the photopigment. To test this hypothesis, we performed reciprocal site-directed mutagenesis of retinochromes from the common bay scallop, *A. irradians*, and the king scallop, *P. maximus*. Using a protein modeling approach, we identified three amino acid sites in the binding pocket and created 14 mutants representing all reciprocal amino acid combinations that occur between the two species at the three sites of interest in each background. Spectral analyses indicate that these three sites have differing degrees of influence on phenotype and appear to have epistatic interactions with other regions of the protein. Our results reveal a more complicated path from genotype to phenotype than typically seen for opsins.

MATERIALS AND METHODS

Retinochrome cloning and insertion into vector

Previously assembled transcriptomes (Serb et al., 2021 preprint) were used to identify retinochrome sequences in *A. irradians* and *P. maximus*. Based on those transcripts, UTR-specific primers were designed to amplify the complete coding regions from cDNA (Table S1). Scallop RNA was extracted from eye tissue using the RiboPure RNA extraction kit (Ambion) and converted to cDNA libraries. PCR was carried out in a 50 µl reaction mixture containing: 5 µl of 10× buffer, 1.5 µl of 25 mmol l^{-1} MgCl, 4 µl of 2.5 mmol l^{-1} dNTPs, 0.2 µl Platinum Taq, 1 µl of 10 µmol l^{-1} of forward and reverse primers (Table S1), and 1 µl of 3 µmol l^{-1} template cDNA. The thermocycler protocol used was as follows, with variation in primer annealing temperatures: 95°C for 2 min; 35 cycles of 95°C for 30 s, primer temperature for 40 s, and 72°C for 2 min; and 72°C for 10 min. PCR products were size-screened using a 1% agarose gel electrophoresis, and bands of the expected size (923 bp) were gel extracted (Qiagen Qiaquick Gel Extraction kit) and cloned using chemically competent *E. coli* cells following the manufacturer's protocol (TOPO TA Cloning Kit with pCR2.1-TOPO). The identity of positive colonies from blue–white screening was confirmed by Sanger DNA sequencing using an ABI 3730

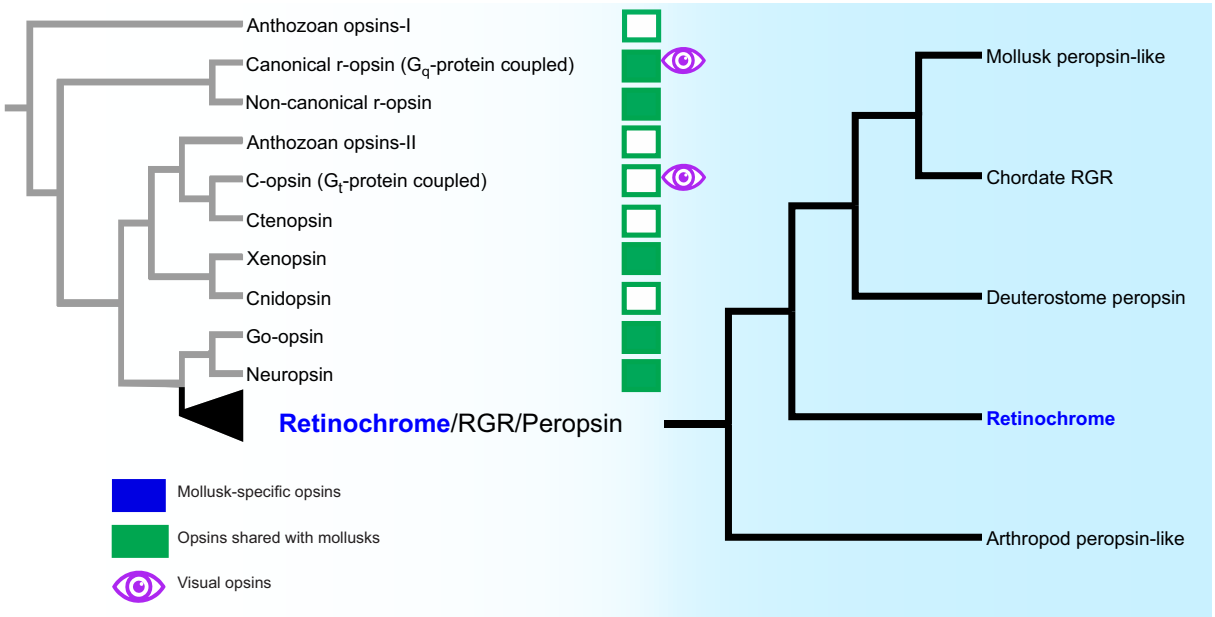

Fig. 1. Representation of evolutionary relationships between major opsin lineages. Redrawn cladogram based on maximum likelihood reconstructions in Ramirez et al. (2016), Vöcking et al. (2017) and Bonadè et al. (2020). Canonical r-opsins (G_q-protein-coupled opsins) are the main visual opsins for invertebrates and c-opsins (G_t-protein-coupled opsins) are the main visual opsins for vertebrates; both are indicated by purple symbols. Opsin lineages shared by mollusks and other taxa are in green. RGR, retinal G-protein-coupled receptor.

Journal of Experimental Biology (2022) 225, jeb242929. doi:10.1242/jeb.242929

Capillary Electrophoresis Genetic Analyzer at the Iowa State University DNA Facility. The genes were then inserted into the expression vector p1D4-hrGFP II (Morrow and Chang, 2010) to generate our working plasmids for retinochrome from *A. irradians* (Airr-RTC) and *P. maximus* (Pmax-RTC). These expression plasmids served as the templates for site-directed mutagenesis.

Modeling and site identification

To identify amino acids lining the binding pocket which may be responsible for altering the λ_{max} of retinochrome, amino acid sequences and predicted 3D models were compared. Amino acid sequences of *A. irradians* retinochrome and *P. maximus* retinochrome were aligned using MAFFT v7.221 (Katoh and Standley, 2013). To identify sites hypothesized to cause changes in the λ_{max} of retinochrome, amino acid sequences of *A. irradians* and *P. maximus* retinochrome were submitted to GPCR-I-TASSER (Zhang et al., 2015) to create 3D models of each protein. The resulting models were then submitted to COACH (Yang et al., 2013a,b), a meta-server used to predict the active interaction sites within protein–ligand interactions. COACH outputs a list of amino acid sites it has predicted to interact with the ligand when bound based on the proximity of the amino acid to the bound ligand model. This list of predicted sites was compared with the alignment of Airr-RTC and Pmax-RTC, specifically to identify predicted interaction sites that are also not conserved sites between the two species, revealing one predicted interaction site which differed between species.

The second approach to identifying amino acids responsible for altering the retinochrome binding pocket environment was based on the role of possible polar interactions between amino acids and variation in the shape or electrostatic environment of the binding pocket. 3D models from COACH were loaded into UCSF Chimera v1.4 (Pettersen et al., 2004), a visualization software for molecular analyses and model comparison. Using Chimera, predicted interaction sites were differentially highlighted based on whether the amino acids were conserved between *A. irradians* and *P. maximus* amino acid sequences. Non-conserved amino acids outside or far from the binding pocket were disregarded, as they are less likely to affect the polarity or shape of the binding pocket. The distances of the predicted interaction sites to the active side chains of non-conserved amino acids were then individually measured. Distances less than 3.5 Å (maximal hydrogen bond length) were searched for, revealing two sites as targets for site-directed mutagenesis.

Site-directed mutagenesis

To create 14 mutants (all possible combinations of the reciprocal mutants at the three sites of interest), the Airr-RTC and Pmax-RTC expression plasmids served as templates for the mutagenesis experiments. DNA Polymerase PfuTurbo (Agilent, Santa Clara, CA, USA) was used for all cloning experiments following the manufacturer's instructions with the same thermocycler profile with varying annealing temperatures dependent on the specifications of each primer set (Table S1). Following the PCR protocol, the reaction product was subjected to a 2.5 h digestion with DpnI (New England Biolabs, Ipswich, MA, USA) at 37°C; 5 µl of the reaction mix was then used to transform TOP10 chemically competent *E. coli* cells (Thermo Fisher Scientific, Waltham, MA, USA). Positive colonies containing the correct mutant sequence were confirmed by Sanger sequencing. Overlapping primers were developed to create mutant Airr-RTC and Pmax-RTC (Table S1). Single mutant primers were used in the creation of all mutants, except for one double mutant plasmid; because of the proximity of the selected sites, a set of primers including two mutation sites was used to guarantee mutation of both sites without removal of either. Mutant products were then used as templates for subsequent mutagenesis. Plasmids were amplified by incubating positively identified colonies in 1 liter liquid LB culture with 50 µg ml^{-1} kanamycin. Plasmids were purified using a HiSpeed Plasmid Maxi Kit (Qiagen, Hilden, Germany) according to the manufacturer's instructions, with the product sequenced to confirm mutant identity.

The seven mutant proteins of Airr-RTC were successfully created, comprising all the combinations of reciprocal mutations at the respective sites. Wild-type Airr-RTC was used as the backbone template for the single mutant proteins. Mutants are labeled with a delta indicating the presence of a mutation followed by the wild-type and resulting amino acid, respectively, flanking the site number: Airr-RTC-ΔM181L, Airr-RTC-ΔY188W and Airr-RTC-ΔV193A. Double mutant proteins used the single mutant retinochromes as a template using the same primers used to create the single mutants; however, because of the proximity of sites 188 and 193, new overhang PCR primers were designed to include the mutations at both sites (Table S1). This ensured the production of a double mutant without the chance of reverse mutation. The resulting mutants are: Airr-RTC-ΔM181L-ΔY188W, Airr-RTC-ΔM181L-ΔV193A, Airr-RTC-ΔY188W-ΔV193A. Finally, the production of the triple mutant was carried out using Airr-RTC-ΔY188W-ΔV193A as the template and the primer set for site 181: Airr-RTC-ΔM181L-ΔY188W-ΔV193A. Reciprocal mutants were made in the same manner using different primers (Table S1) to create the respective combinations of mutants with Pmax-RTC: Pmax-RTC-ΔL181M, Pmax-RTC-ΔW188Y and Pmax-RTC-ΔA193V, Pmax-RTC-ΔL181M-ΔW188Y, Pmax-RTC-ΔL181M-ΔA193V and Pmax-RTC-ΔW188Y-ΔA193V, and Pmax-RTC-ΔL181M-ΔW188Y-ΔA193V.

Cell culture, expression and pull-down

To express wild-type and mutant retinochrome proteins *in vitro*, 15 plates (Corning Falcon Standard Tissue Culture Dishes, 10 cm, ref. 353003, Tewksbury, MA, USA) of confluent HEK293T cells (ATCC, Manassas, VA, USA) were transfected with 8 µg DNA and 20 µl 293fectin Transfecting Reagent (Thermo Fisher Scientific) per plate, according to the manufacturer's instructions. Bovine rhodopsin was used as a system control using two plates of confluent HEK293T cells with equivalent amounts of DNA and 293fectin as described above. Plates were incubated for 24 h before the minimum essential medium (MEM) was exchanged with new MEM containing 5 µmol of all-*trans* retinal for retinochrome and 5 µmol of 11-*cis* retinal for bovine rhodopsin. Because of the addition of light-sensitive retinal at this step, all subsequent culturing and experimentation was conducted in a dark-lab environment under dim red light. The plates were incubated for another 24 h before cells were harvested by scraping the plates twice with 5 ml buffer A (3 mmol $MgCl_2$, 140 mmol NaCl, 50 mmol Hepes pH 6.6, 10 mg ml^{-1} aprotinin and 10 mg ml^{-1} leupeptin). All subsequent centrifugation and incubation steps were at 4°C or on ice. Cells were collected by pellet following centrifugation (10 min at 1620 relative centrifugal force, RCF) and resuspended in 10 ml buffer A. Cells were washed 2 times in total following the same protocol.

After the second wash, cells were resuspended in 2 ml per plate of buffer A with 5 µmol all-*trans* retinal to regenerate the

Journal of Experimental Biology (2022) 225, jeb242929. doi:10.1242/jeb.242929

photopigment. The cell suspension was nutated for 1 h at 4°C. The regenerated cells were pelleted by centrifugation for collection at 38,360 RCF for 20 min and resuspended in solubilization buffer (buffer A plus 1% *n*-dodecyl β-D-maltoside and 20% w/v glycerol) using 1 ml solubilization buffer per plate. The solubilized cells were nutated for 1 h at 4°C. After the 1 h nutation, the mixture was centrifuged for 20 min at 42,740 RCF. The supernatant was then added to a 100 ml slurry resin (1:1 v/v resin/resin buffer) composed of 1D4 antibody (University of British Columbia, Canada) conjugated to Sepharose beads and nutated for 30 min. The resin was washed 3 times with 5 ml washing buffer (buffer A with 1% *n*-dodecyl β-D-maltoside and 20% w/v glycerol without aprotinin and leupeptin), and the protein was eluted with 2 ml elution buffer (washing buffer with 40 mmol Rho1D4 peptide TETSQVAPA; dapted from Oprian et al., 1987). To concentrate the protein sample, eluate was concentrated to ∼300 µl using 4 Amicon Ultra 0.5 ml 10 kDa centrifugal filters (Millipore, Billerica, MA, USA).

Spectrophotometry

Ultraviolet-visible absorption spectra (250–750 nm) of purified proteins were measured at 15°C using a Hitachi U-3900 spectrophotometer (Chiyoda, Tokyo, Japan). Data analysis was performed on the mean value of five spectral measurements with the software UV Solutions v4.2 (Hitachi). To test the proteins for photoreactivity, 'dark' absorbance was measured first for each protein, e.g. the naive protein that had been incubated and regenerated with the all-*trans* retinal chromophore. Retinochrome proteins were tested independently with all-*trans* retinal because (1) retinochrome preferentially binds all-*trans* retinal (Hara and Hara, 1967) and (2) retinochrome forms a stable pigment only in the presence of all-*trans* retinal (Faggionato and Serb, 2017). The maximum absorbance of the all-*trans* retinal when unbound to retinochrome apoprotein is 380 nm. Thus, any light-dependent isomerization converting free all-*trans* retinal to 11-*cis* retinal will be undetectable in the experimental system. Therefore, the most plausible explanation for any observed change in spectral absorbance is that it is due to a conformational change of the retinal covalently bonded to the apoprotein.

For the 'light' spectra, extracted proteins were bleached at different wavelengths according to λ_{max} identified from the 'dark' spectra and then the absorbance was measured. Extracted proteins were first exposed to light at ∼474 nm using two blue LEDs (MR16-B24-15-DI; superbrightleds.com) simultaneously irradiating both transparent sides of the cuvette (Hellma Analytics 104002B-10-40, Müllheim, Germany) for 3 min and the absorbance was recorded. A final exposure to white light was performed, followed by an absorbance measurement. Mean spectra were plotted using R scripts (http://www.R-project.org/) with interpolation of the data points being performed with the R function smooth.spline.

A differential spectrum was calculated from two adjacent light treatments [i.e. the absorbance spectrum before exposure to light (dark spectra) was subtracted from spectra after the exposure to blue light(blue spectra)] and tested for fit to an A1 rhodopsin mathematical template (Gačić et al., 2019) using the Curve Fitting Toolbox in MATLAB (*fittype, fit*; The MathWorks, Natick, MA, USA). Each difference spectrum was tested against templates with λ_{max} ranging from 350 nm to 750 nm at 1 nm intervals. Prior to fitting the template, the minimum baseline value of each differential spectrum was set to zero and the curve was normalized to the peak value in the visible spectrum. The best fit was determined by the least sum of squares deviations from 25 nm below the peak to 75 nm above. Most of the evaluated spectra were excellent fits to the template (R^2>0.75). For spectra with poor fits (R^2<0.50) as a result of baseline artifacts in the blue treatment, the template was fitted using a narrower range of λ_{max} templates (25 nm below the peak to 5 nm above).

This approach minimized the likelihood of observed differences in spectrum being a result of unrelated factors such as handling of the cuvette between light exposures and absorbance measurements or degradation of the protein sample other than through light treatments themselves. These methods were carried out for the wild-type proteins of *A. irradians* and *P. maximus* and then the seven mutant *A. irradians* proteins and seven mutant *P. maximus* proteins.

RESULTS

Retinochromes have a similar sequence but differ spectrally between scallop species

The cloned retinochrome sequences of *A. irradians* (GenBank KX550908) and *P. maximus* (GenBank XM_033877948.1) were 308 amino acids. The two protein sequences were 92% similar, with 25 different amino acid residues. There was high sequence conservation within the binding pocket (99%), and most of the residue differences belonged to the same biochemical class. Residues surrounding sites important for the function of retinochrome, such as the lysine for chromophore binding and the glutamate counterion, are conserved between scallop samples, as are amino acids around these sites, and correspond to the bovine numbering system positions 296 and 181, respectively (Fig. S1).

To determine the λ_{max} of *A. irradians* retinochrome (Airr-RTC) and *P. maximus* retinochrome (Pmax-RTC), we expressed both proteins in HEK293T cells and incubated them with all-*trans* retinal. The λ_{max} of Airr-RTC was 525 nm (Fig. 2A, black curve), while that of Pmax-RTC was 496 nm (Fig. 2C, black curve). This is the first *in vitro* measurement of retinochrome λ_{max} from a scallop species, and our measurements are consistent with prior studies conducted on retinochrome isolated in crude extracts from squid (Hara and Hara, 1982) and snail (Ozaki et al., 1986) and expressed *in vitro* from squid (Terakita et al., 2000). Unfitted spectral data are shown in Figs S2 and S3.

Three amino acid changes indicate potential interaction sites lining the retinal binding pocket

To narrow down the candidate list of 25 spectral tuning sites, we employed 3D protein models to identify potential ligand interaction sites. In total, 18 positions were identified between the two retinochrome models and were at the same binding pocket locations of two RTC homologs with two exceptions. Positions 170 and 188 were only predicted to be interaction sites in the Pmax-RTC model, not in the Airr-RTC model (Fig. 3A,B). However, the amino acid residue was conserved at position 170 and thus was removed from the candidate list. In contrast, position 188 varied between a tryptophan in Pmax-RTC versus a tyrosine in Airr-RTC. While both of these amino acids are classified as hydrophobic with similar pK_a scores, the position of the tyrosine's hydroxyl group could allow a more direct polarity change in the binding pocket (Shimono et al., 2001), and therefore may affect the absorbance of the photon by the bound retinal (Fig. 3C). We selected site 188 as the first site for mutation.

To identify other sites that may be responsible for altering the shape of or electrostatic environment within the binding pocket, we compared the 3D models of the Airr-RTC and Pmax-RTC focusing on the location of the non-conserved amino acids. We used UCSF Chimera to manipulate the 3D models, allowing us to measure the distance between active groups of the amino acid residues of interest

Journal of Experimental Biology (2022) 225, jeb242929. doi:10.1242/jeb.242929

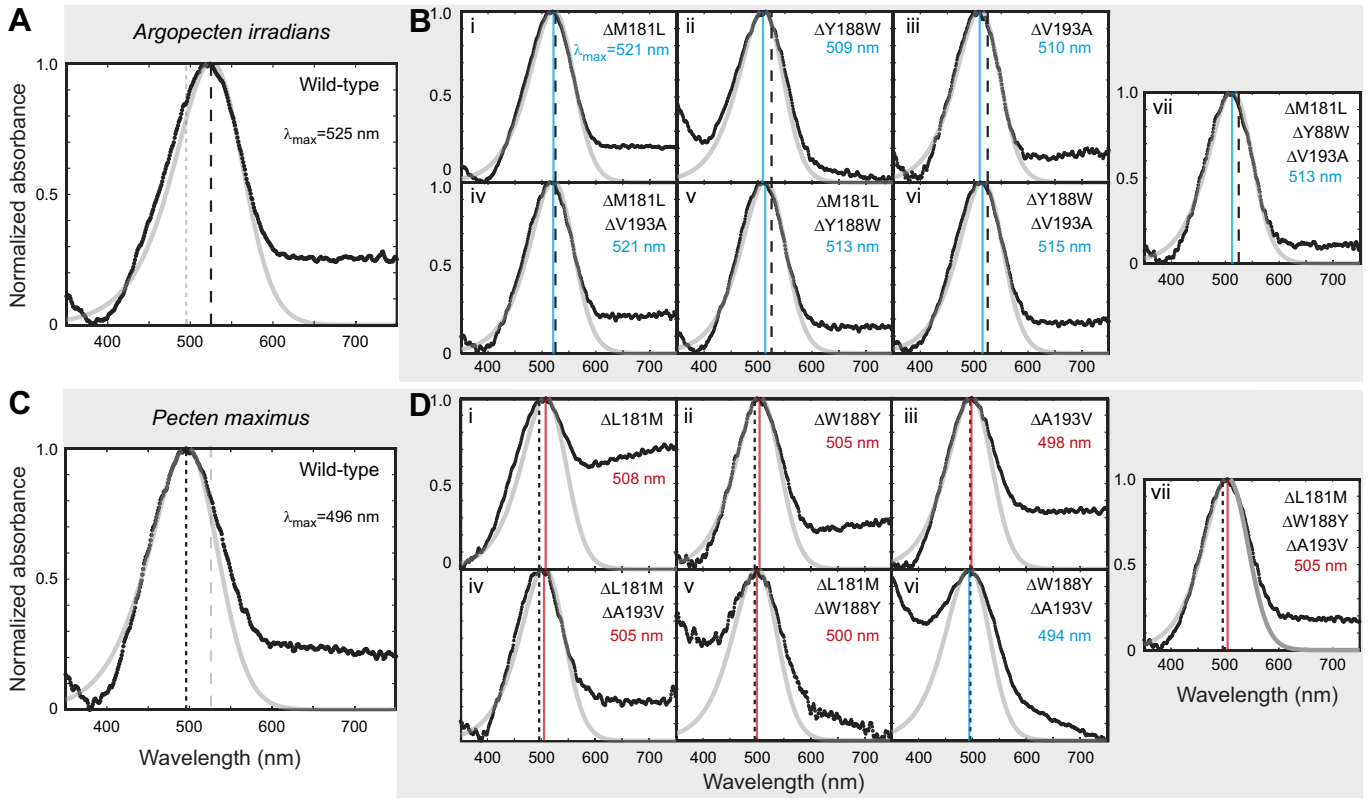

Fig. 2. Site-directed mutagenesis in *Argopecten irradians* and *Pecten maximus* retinochromes causes spectral shifts. Difference absorption spectra of dark- and blue-light-treated retinochromes generated through heterologous expression (black traces), fitted to an A1 visual pigment template (thick gray curve). Spectra were measured at 15°C. (A,C) Wild-type retinochrome absorption spectra for each species. Vertical black dashed lines represent λ_{max} for the template fitted to each wild-type species. For ease of species comparisons, the vertical gray dashed line in A denotes *P. max* λ_{max} and the vertical gray dashed line in C denotes *A. irradians* λ_{max}. (B,D) Summary of data from each mutant retinochrome. Single mutations are shown in i–iii; double mutations in iv–vi; and triple mutations in vii. Specific mutation sites in indicated in the upper right corner. λ_{max} of the template fitted to each spectrum is given in blue or red text below the mutation and denoted as a solid vertical line in the plot. Blue represents blue-shifted λ_{max} (relative to wild-type); red represents red-shifted λ_{max}. The wild-type λ_{max} line (vertical black dashed line) for each species is also shown to indicate the shift induced in each mutant.

in relation to one another as well as the retinal molecule. Many non-covalent polar interactions range from 0.5 to 3.5 Å; thus, this range was used as a criterion for identifying sites of interest through bond measurements. Site 184 (Fig. 3A,B) is a conserved methionine in both Pmax-RTC and Airr-RTC but was predicted by COACH to function as a ligand interaction site. A neighboring site which is not conserved is site 181. Site 181 is a methionine in Airr-RTC and a leucine in Pmax-RTC. The primary difference between these non-polar side chains is the presence of the thioether of the methionine. This thioether allows for oxidation of the residue and acts as a strong hydrogen bond acceptor. Bond measurements show that the sulfur of Met181 is only 2.85 Å from the side chain hydrogens of Met184 (Fig. 3C). We selected site 181 as a second site of interest because of its potential to change the polarity of an amino acid lining the binding pocket, site 184.

Using the same logic, we also identified non-conserved position 193 as a site of interest. Position 189, a leucine, was predicted by COACH as an interaction site for the ligand (Fig. 3A,B), yet was conserved between the RTC homologs. However, within 0.5 to 3.5 Å, position 193 differed as a valine in Airr-RTC or an alanine in Pmax-RTC. The isopropyl group of the valine is much bulkier than that of the methyl group found in alanine. Given the proximity of the hydrogens found on the carbon groups of the leucine to those of the valine (between 2.735 Å and 3.202 Å), it is likely that the location of predicted interaction site 193 is altered in the space of the protein (Fig. 3C).

Selected amino acid mutations cause shifts in λ_{max}

Single mutations had specific effects on λ_{max} in comparison to the Airr-RTC and Pmax-RTC wild-type proteins (Table 1). In Airr-RTC single mutants, site 181 (M181L) absorbed at 521 nm, a −4 nm change from the wild-type (Fig. 2Bi), while site 188 (Y188W) and site 193 (V193A) resulted in a blue shift of either 16 or 15 nm (λ_{max} of 509 nm and 510 nm), respectively (Fig. 2Bi–iii). The blue shift from mutations at 188 and 193 suggests their role as spectral tuning sites. Both double mutants containing mutations in site 188 (Airr-RTC-ΔM181L-ΔY188W and Airr-RTC-ΔY188W-ΔV193A) also shifted blue, with λ_{max} of 513 nm and 515 nm, respectively (Fig. 2Bv,vi). The double mutations at sites 181 and 193 had little change in the absorbance peak from the wild-type with a λ_{max} of 521 nm (Fig. 2Biv) in the Airr-RTC background. Considering the λ_{max} of the single mutants at sites 181 and 193, the combination of the two shows the effects at site 181 either compensate for or outweigh the effects at site 193. The triple mutant (Airr-RTC-ΔM181L-ΔY188W-ΔV193A) resulted in a 12 nm blue shift (λ_{max}=513 nm) (Fig. 2Bvii).

We also expressed and recorded the spectra of the seven mutant Pmax-RTC (Fig. 2D). From the single mutants, sites 181 (Leu to Met) and 193 (Ala to Val) showed a slight red shift with λ_{max} of 508 nm and 498 nm, respectively (Fig. 2Di,iii). Site 188 (Trp to Tyr) showed a red shift to 505 nm (Fig. 2Dii). The Pmax-RTC double mutants had no or little change in λ_{max} from wild-type spectra. Double mutant protein Pmax-RTC- ΔM181L-ΔY188W had

Journal of Experimental Biology (2022) 225, jeb242929. doi:10.1242/jeb.242929

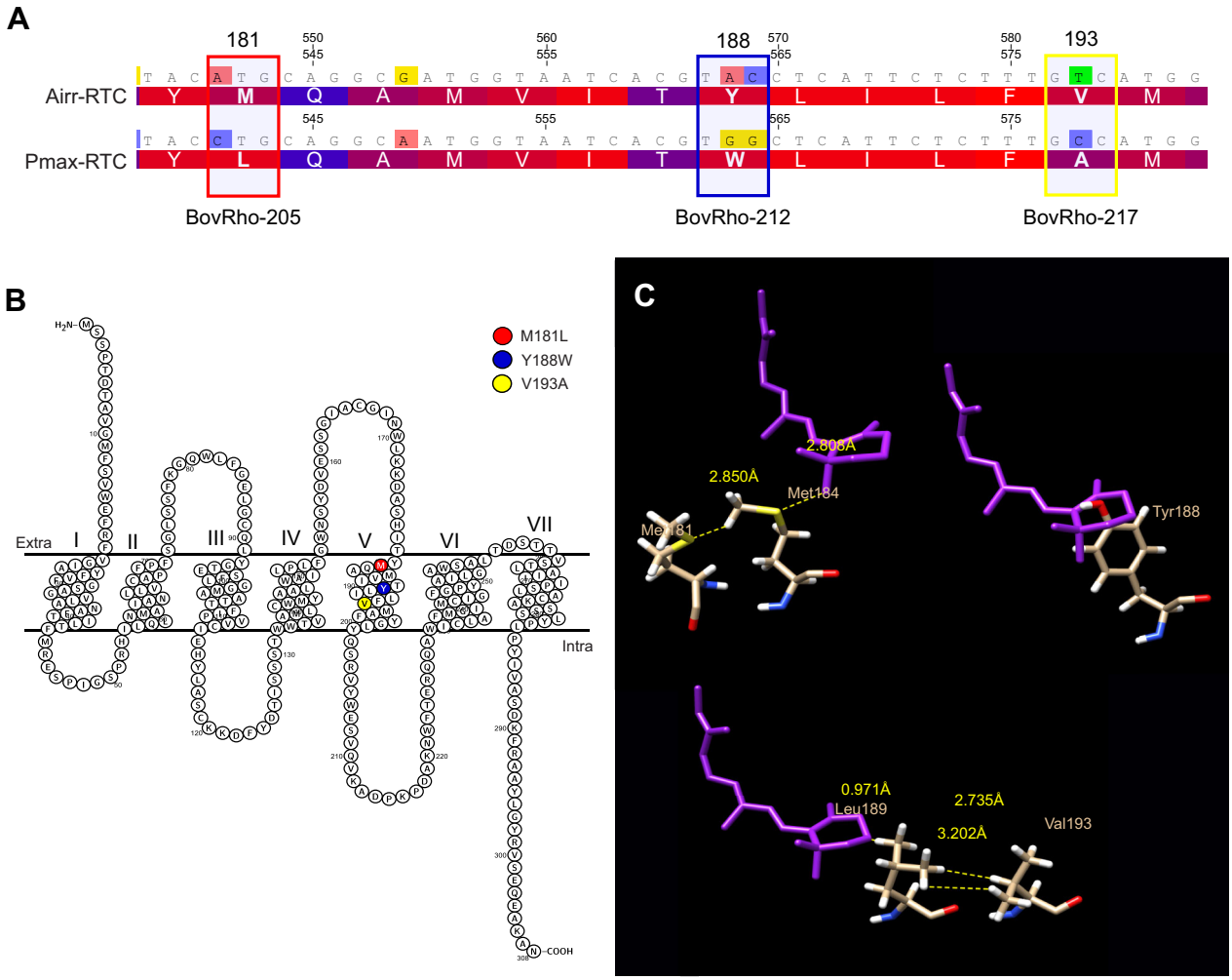

Fig. 3. Location of candidate spectral tuning sites in retinochrome. (A) Amino acid and nucleotide sequence alignments of retinochrome for *A. irradians* (Airr-RTC) and *P. maximus* (Pmax-RTC) with nucleotide substitutions shaded. Above the alignment, large numbers are amino acid sites; small numbers are nucleotide positions of the coding sequence. Numbers below the alignment correspond to the numbering system of bovine rhodopsin (see Fig. S1 for full alignment). Amino acids are colored by the degree of hydrophobicity of the side chains ranging from red (more hydrophobic) to blue (less hydrophobic). Colored boxes highlight the three amino acid differences between Airr-RTC and Pmax-RTC at sites with predicted involvement in spectral tuning and target nucleotide positions for mutagenesis. (B) Snakeplot showing the secondary structure of Airr-RTC. The sites of the mutagenesis experiments are highlighted in red (M181), blue (Y188) and yellow (V193). Seven transmembrane helices are indicated by roman numerals. (C) 3D modeling of bound retinal chromophore and sites of interest. The 11-*cis* retinal molecule is purple, with the amino acid chains colored by atom composition. Yellow dashed lines and numbers indicate the distances between structures. Amino acid residue identities and location are labeled in beige next to the residue.

a λ_{max} of 500 nm, the combination mutant Pmax-RTC- ΔM181L-ΔV193A showed a change in λ_{max} from the wild-type protein at 505 nm, and Pmax-RTC-ΔY188W-ΔV193A had a λ_{max} of 494 nm (Fig. 2Div–vi). The triple mutant Pmax-RTC-ΔM181L-ΔY188W-ΔV193A also showed a 5 nm red shift (λ_{max}=505 nm; Fig. 2Dvii).

DISCUSSION

The relationship between genotype and phenotype is a central unanswered question in biology. Here, we provide the first experimental results with respect to absorbance spectra of a molluscan photopigment. We investigated the genotype–phenotype relationship by comparing retinochrome from two closely related scallop species and, through site-directed mutagenesis experiments, altered amino acids predicted to influence spectral absorbance. Because the *A. irradians* and *P. maximus* retinochrome sequences are highly conserved around both the Schiff base binding site and the counterion (Fig. S1), the 29 nm difference in retinochrome λ_{max} that we observed between the two species must be attributed to non-conserved sites elsewhere in the protein. We hypothesized that amino acids lining the binding pocket may in part be responsible for spectral tuning of retinochrome λ_{max}. We used bioinformatic methods to identify three non-conserved amino acids that may alter the shape or electrostatic environment of the opsin binding pocket, and reciprocally mutated those sites between *A. irradians* and *P. maximus* to test their role in spectral tuning. These three sites are, in part, responsible for spectral tuning of scallop retinochromes. However, our results show that the relationship between amino acid changes and spectral shifts is not simply additive, and indicate a role of intramolecular epistasis in retinochrome spectral tuning.

Predicted ligand interaction sites alter λ_{max}

Through protein modeling and subsequent testing of 14 reciprocal site-directed mutants, we found three sites that effect spectral tuning of retinochrome. However, these results were not always predictable or additive in nature. Site 188, a tyrosine in *A. irradians* and a

Journal of Experimental Biology (2022) 225, jeb242929. doi:10.1242/jeb.242929

Table 1. Mutant retinochrome λ_{max} values and the difference between mutant and wild-type λ_{max} values

	Airr-RTC λ_{max}=525 nm			Pmax-RTC λ_{max}=496 nm	
Mutation position (Airr to Pmax)	Maximum absorbance (nm)	Shift from wild-type (nm)*	Mutation position (Pmax to Airr)	Maximum absorbance (nm)	Shift from wild-type (nm)*
181 (M to L)	521	−4	181 (L to M)	508	+12
188 (Y to W)	509	−16	188 (W to Y)	505	+9
193 (V to A)	510	−15	193 (A to V)	498	+2
181+188	513	−12	181+188	500	+4
181+193	521	−4	181+193	505	+9
188+193	515	−10	188+193	494	−2
181+188+193	513	−12	181+188+193	505	+9

*Positive numbers indicate a red shift from wild-type; negative numbers are a blue shift from wild-type.

tryptophan in *P. maximus*, was the only non-conserved predicted interaction site based on the COACH analysis. Mutations created at this site resulted in a −16 nm blue shift and a +9 nm red shift of λ_{max} for Airr-RTC-ΔY188W and Pmax-RTC-ΔW188Y, respectively. This mirroring effect between reciprocal mutants strongly indicates an independent effect on spectral tuning at this location. The impact of hydroxyl-containing amino acids, such as tyrosine, on λ_{max} is well documented in both vertebrate and invertebrate photopigments (Merbs and Nathans, 1993; Frentiu et al., 2015; Shimono et al., 2001; Nakayama and Khorana, 1991). Such studies demonstrate that the change in λ_{max} is due to the potential dipole moments created by the oxygen of hydroxyl groups in the proximity of the β-ionone ring of the chromophore, which cause a red shift of the absorption maximum or dipole residues around the protonated Schiff base that results in a λ_{max} shift in the opposite direction (e.g. OH-site rule; Sekharan et al., 2012). The former may be occurring in Pmax-RTC-ΔW188Y. Our Airr-RTC 3D model shows the tyrosine hydroxyl group inserted into the aromatic ring of retinal, while the tryptophan in the Pmax-RTC model does not extend as far. This impossible orientation of tyrosine is likely the result of the software's limitation, which only provides 11-*cis* retinal as a ligand option, rather than the all-*trans* retinal preferred by retinochrome. The straight poly-carbon chain of the all-*trans* retinal would likely rest differently in the binding pocket of retinochrome, but the potential for dipole moments from the hydroxyl group could still affect the electrostatic environment of the binding pocket. This hydroxyl group is absent in the tryptophan at site 188 of wild-type *P. maximus*. Spectral analyses of the single, double and triple mutants of Airr-RTC with the Y188W mutation all had a blue shift in λ_{max} ranging from −10 nm to −16 nm as expected under the OH-site rule, while spectra of the Pmax-RTC single, double and triple mutants with the W188Y mutation did not show the reciprocal pattern. The Pmax-RTC W188Y single mutant, L181M and W188Y double mutant, and L181M, W188Y and A193V triple mutant had slight red shifts between +4 nm and +9 nm, while the double mutant containing W188Y and A193V showed a blue shift of 2 nm. These conflicting changes in λ_{max} indicate that other polar groups may be involved in retinochrome spectral tuning. Future work should consider the 'dipole-orientation rule', an extension of the OH-site rule, that takes into account both the location and orientation of polar groups, including water molecules, in modeling approaches (Jiang et al., 1993).

The remaining two mutant sites, 181 and 193, allowed us to investigate the effects of residues in close proximity to predicted interaction sites rather than sites directly interacting with the retinal chromophore. The results of our site-directed mutagenesis experiments point to a hierarchy of effects. For instance, we observed the same −4 nm (λ_{max}=521 nm) shift in Airr-RTC with the M181L single mutation as with the double mutant with M181L and V193A, yet the single mutant V193A had a large −15 nm blue shift (λ_{max}=510 nm). The lack of spectral shift in the double mutant between these sites indicates that the effect of M181L may compensate for the alteration caused by the mutation at V193A in the Airr-RTC backbone. In Pmax-RTC mutants, single mutants at the same sites, L181M and A193V, had the reverse magnitude (+12 nm and +2 nm, respectively), while the double mutant of those sites had an intermediate change in λ_{max} (+9 nm). This red shift was maintained in Pmax-RTC mutants at the same sites. The mutation with hydrophobic residues in bacterial rhodopsins has been shown to cause dramatic blue shifts (up to 80 nm relative to wild-type) (Greenhalgh et al., 1993), because the side chains of these hydrophobic residues tend to be bulky as a result of the saturation of hydrogens and may restrict movement of retinal's β-ionone ring. Thus, the presence of hydrophobic residues may alter the binding pocket geometry by pushing adjacent residues, such as those lining the binding pocket, into different orientations.

A possible role for binding pocket shape in determining λ_{max}

The mutation V193A in Airr-RTC may exhibit a stronger effect on the shape of the binding pocket. Airr-RTC mutants containing V193A showed large blue shifts (−10 to −15 nm), with the exception of the double mutant also containing M181L, which showed a slight −4 nm blue shift. The decrease in size of side chains from valine to alanine may be significant enough to reduce the bulging effect of this amino acid residue on the proposed ligand binding site, creating variation in the region of the protein and the shape or size of the binding pocket. However, when combined with the M181L mutation, the small change of λ_{max} could suggest that the second mutation compensates for the effect of V193A. Reciprocal mutants at site 193 in Pmax-RTC (A193V) were expected to result in red shifts, mirroring those of Airr-RTC mutants. The smallest shift was the single A193V mutant (+2 nm) and the double Pmax-RTC-ΔL181M-ΔW188Y mutant (+4 nm). Here, the increase in side chain bulk (A to V) producing the relatively small change to λ_{max} may indicate a weakening of the interaction between the ligand and retinochrome.

A scenario where mutations in the binding pocket weaken the interactions with the chromophore may arise from changes in the distance between the amino acids in the binding pocket and the bound retinal as well as the distance between interacting amino acids. A change in distance can alter the strength of the interactions of these components, thus potentially changing the polar environment of the binding pocket and the λ_{max} of the protein. While mutations in Airr-RTC cause a blue shift towards the wild-type λ_{max} of Pmax-RTC, the λ_{max} of the reciprocal mutants in Pmax-RTC do not change with the same magnitude. This may actually

reflect a reduced interaction strength between binding pocket residues and the chromophore. Being able to visualize the protein and binding pocket shape via the crystal structure would help us to understand how the shape is affected by specific mutations.

Epistatic effect on spectral tuning

In numerous vertebrate visual opsins, spectral tuning is attributed to one or a few amino acid substitutions (Hunt et al., 2009). For example, three amino acids are responsible for red shifting in the evolution of old world primate trichromatic vision via additive effects (Surridge et al., 2003; Neitz et al., 2016; but see Chan et al., 1992). We therefore had reason to expect one or particular combinations of the three predicted sites for spectral tuning to be sufficient for shifting λ_{max} from one homolog to the other. However, our reciprocal site-directed mutagenesis rarely mirrored the spectral tuning between Airr-RTC and Pmax-RTC backgrounds. In fact, site 188 was the only mutant with similar blue and red shifts for Airr-RTC (−16 nm) and Pmax-RTC (+9 nm), respectively, relative to their wild-type proteins.

Both triple mutants had λ_{max} shifts in the expected direction, though neither shift had a magnitude great enough to match the wild-type λ_{max} of the other species, e.g. Airr-RTC-ΔM181L-ΔY188W-ΔV193A λ_{max} did not match the Pmax-RTC λ_{max}. Otherwise, the spectral changes for the double and triple mutant retinochromes relative to the wild-type generally did not reflect additive changes of the single mutant effects. Together, these results indicate that amino acid substitutions in these spectral tuning sites may experience epistatic effects, the non-additive effect on protein function arising from identical amino acid substitutions in different genetic backgrounds. Intramolecular epistasis has been implicated in opsin evolution, likely resulting from trade-offs between selection maintaining protein stability and spectral tuning (Dungan and Chang, 2017; Castiglione and Chang, 2018). Selection on amino acid sites relating to properties unrelated to spectral tuning in retinochrome may therefore hinder our ability predict changes to absorbance from these three residues alone.

Scallop retinochrome as a promising model for understanding opsin function

In this study we were able to identify and successfully mutate three amino acid sites that affect absorption maxima in scallop retinochrome. Our results demonstrate that retinochrome is easy to clone, mutate and express in heterologous cell culture, making it a promising model to examine the genotype–phenotype relationship in opsins. To make retinochrome a more powerful system, we need detailed atomic-level information to better model how all-*trans* retinal interacts with the protein and more extensive sampling across molluscan species to describe the natural variants and patterns of molecular evolution. This study and others (Nathans, 1990; Yokoyama et al., 2014, 2015) have shown that the amino acid sequence does not provide a reliable predictor of λ_{max} trends. In fact, λ_{max} values are likely determined by changes in the topographical distribution and orientation of the amino acid side chains surrounding the chromophore, making 3D structure of the photopigment essential. The application of QM/MM models is a powerful tool for studying proteins beyond their structural characterization (Melaccio et al., 2012; Hirayama et al., 1994; Andruniów et al., 2004; Coto et al., 2006). However, the modeling of opsin proteins is particularly challenging as it requires not only an atomic-level representation to correctly describe the interaction between the chromophore and its environment but also a correct description of its light-responsive electronic structure. Integrating experimental measurements of retinochrome mutants with model refinements could yield more accurate and consistent QM/MM models. With such tools, it will be possible to classify the effect of different non-covalent interactions, construct a topographical map of their distribution and, ultimately, develop hypotheses on how the λ_{max} values and reactivity properties of the photopigment respond to these interactions (Gozem et al., 2014).

Conclusions

We demonstrate the first example of expression, mutagenesis and spectral analysis of retinochrome from scallop species. We showed that the absorbance peaks of scallop retinochromes fall within the blue–green range of the visible spectrum similar to *in vivo* measurements of cephalopod retinochrome (Terakita et al., 2000). We propose methods to identify amino acid sites potentially responsible for the spectral tuning of photopigments. Amino acids near sites of import, such as the Schiff base binding site and counterion, have long been recognized for their role in spectral tuning, but our results show that sites elsewhere in the protein may be responsible for tuning of the λ_{max}. While we uncovered sites for spectral tuning, we rarely observed mirrored changes in λ_{max} for our reciprocal mutagenesis studies, suggesting that retinochrome function may be influenced by epistasis, thus complicating the predictability of genotype to phenotype relationships for this opsin. Finally, our findings highlight the effectiveness of scallop retinochrome as a model system for investigating the relationship between genotype and phenotype of photopigments.

Acknowledgements

We thank Rosalie Crouch (Storm Eye Institute, Medical University of South Carolina) and the National Eye Institute for supplying 11-*cis*-retinal, Belinda Chang for providing the expression vector p1D4-hrGFP II, and Julia Sigwart for scallop specimens. We are indebted to Davide Faggionato, who developed the heterologous expression method for scallop opsins. We thank two anonymous reviewers for their helpful comments and suggestions to the manuscript. We are grateful to the Serb lab for comments on earlier drafts, in particular Jorge Audino, who created Fig. 1. This study is part of G.D.S.'s PhD thesis through the Graduate Program in Interdepartmental Genetics and Genomics (Iowa State University).

Competing interests

The authors declare no competing or financial interests.

Author contributions

Conceptualization: G.D.S., J.M.S.; Methodology: G.D.S., J.M.S.; Formal analysis: K.D.F.; Investigation: G.D.S., K.E.M.; Resources: J.M.S.; Writing - original draft: G.D.S.; Writing - review & editing: K.E.M., K.D.F., J.M.S.; Visualization: K.D.F.; Supervision: J.M.S.; Project administration: J.M.S.; Funding acquisition: J.M.S.

Funding

This work was supported by an Iowa State University Bailey Research Career Development Award (to J.M.S.). Open access funding provided by Iowa State University. Deposited in PMC for immediate release.

Data availability

Wild type DNA sequences (*n*=2) have been deposited in GenBank: KX550908, XM_033877948.1 (CDS) and XP_033733839.1 (protein).

References

Andruniów, T., Ferre, N. and Olivucci, M. (2004). Structure, initial excited-state relaxation, and energy storage of rhodopsin resolved at the multiconfigurational perturbation theory level. *Proc. Natl. Acad. Sci. USA* **101**, 17908-17913. doi:10.1073/pnas.0407997101

Asenjo, A. B., Rim, J. and Oprian, D. D. (1994). Molecular determinants of human red/green color discrimination. *Neuron* **12**, 1131-1138. doi:10.1016/0896-6273(94)90320-4

Beppu, Y. (1997). Theoretical study of color control mechanism in retinal proteins: orientational effects of aromatic amino acid residues upon opsin shift. *J. Phys. Soc. Jpn.* 66, 3303-3309.

Beppu, Y. and Kakitani, T. (1994). Theoretical study of color control mechanism in retinal proteins. *Photochem. Photobiol.* **59**, 660-669. doi:10.1111/j.1751-1097.1994.tb08235.x
Bonadè, M., Ogura, A., Corre, E., Bassaglia, Y. and Bonnaud-Ponticelli, L. (2020). Diversity of light sensing molecules and their expression during the embryogenesis of the Cuttlefish (Sepia officinalis). *Front. Physiol.* **11**, 1-21. doi:10.3389/fphys.2020.521989
Castiglione, G. M. and Chang, B. S. W. (2018). Functional trade-offs and environmental variation shaped ancient trajectories in the evolution of dim-light vision. *eLife* **7**, 1-30. doi:10.7554/eLife.35957
Chan, T., Lee, M. and Sakmar, T. P. (1992). Introduction of hydroxyl-bearing amino acids causes bathochromic spectral shifts in rhodopsin. Amino acid substitutions responsible for red-green color pigment spectral tuning. *J. Biol. Chem.* **267**, 9478-9480. doi:10.1016/S0021-9258(19)50115-6
Clarke, A. H. (1965). The scallop superspecies Aequipecten irradians (Lamarck). *Macalogia* **2**, 161-188.
Coto, P. B., Strambi, A., Ferré, N. and Olivucci, M. (2006). The color of rhodopsins at the ab initio multiconfigurational perturbation theory resolution. *Proc. Natl. Acad. Sci. USA* **103**, 17154-17159. doi:10.1073/pnas.0604048103
Duncan, P. F., Brand, A. R., Strand, Ø. and Foucher, E. (2016). The European Scallop Fisheries for Pecten maximus, Aequipecten opercularis, Chlamys islandica, and Mimachlamys varia. *Dev. Aquac. Fish. Sci.* **40**, 781-858. doi:10.1016/B978-0-444-62710-0.00019-5
Dungan, S. Z. and Chang, B. S. W. (2017). Epistatic interactions influence terrestrial–marine functional shifts in cetacean rhodopsin. *Proc. R. Soc. B Biol. Sci.* **284**. doi:10.1098/rspb.2016.2743
Faggionato, D. and Serb, J. M. (2017). Strategy to identify and test putative light-sensitive non-opsin G-protein-coupled receptors: A case study. *Biol. Bull.* **233**, 70-82. doi:10.1086/694842
Ferré, N. and Olivucci, M. (2003). Probing the rhodopsin cavity with reduced retinal models at the CASPT2/CASSCF/AMBER level of theory. *J. Am. Chem. Soc.* **125**, 6868-6869.
Frentiu, F. D., Yuan, F., Savage, W. K., Bernard, G. D., Mullen, S. P. and Briscoe, A. D. (2015). Opsin clines in butterflies suggest novel roles for insect photopigments. *Mol. Biol. Evol.* **32**, 368-379. doi:10.1093/molbev/msu304
Gačić, Z., Mićković, B., Gačić, L. and Damjanović, I. (2019). New spectral templates for rhodopsin and porphyropsin visual pigments. *Arch. Biol. Sci.* **71**, 103-110. doi:10.2298/ABS180822052G
González-Luque, R., Garavelli, M., Bernardi, F., Merchán, M., Robb, M. A. and Olivucci, M. (2000). Computational evidence in favor of a two-state, two-mode model of the retinal chromophore photoisomerization. *Proc. Natl. Acad. Sci. USA* **97**, 9379-9384. doi:10.1073/pnas.97.17.9379
Gozem, S., Melaccio, F., Luk, H. L., Rinaldi, S. and Olivucci, M. (2014). Learning from photobiology how to design molecular devices using a computer. *Chem. Soc. Rev.* **43**, 4019-4036. doi:10.1039/c4cs00037d
Greenhalgh, D. A., Farrens, D. L., Subramaniam, S. and Khorana, H. G. (1993). Hydrophobic amino acids in the retinal-binding pocket of bacteriorhodopsin. *J. Biol. Chem.* **268**, 20305-20311. doi:10.1016/S0021-9258(20)80729-7
Hara, T. and Hara, R. (1967). Vision in Octopus and Squid: Rhodopsin and Retinochrome in the Squid Retina. *Nature* **214**, 573-575. doi:10.1038/214573a0
Hara, T. and Hara, R. (1968). Regeneration of Squid Retinochrome. *Nature* **219**, 450-454. doi:10.1038/219450a0
Hara, T. and Hara, R. (1982). Cephalopod Retinochrome. *Photochem. Vis.* **81**, 190-197. doi:10.1016/S0076-6879(82)81031-8
Hara, T., Hara, R. and Takeuchi, J. (1967). Rhodopsin and Retinochrome in the Octopus Retina. *Nature* **214**, 572-573. doi:10.1038/214572a0
Hara, T., Hara, R., Hara, N. I., Nishimura, M., Terakita, A. and Ozaki, K. (1992). The rhodopsin-retinochrome system in the squid visual cell. Colloque INSERM; Structures et fonctions des retino proteines Colloquium; Structures and functions of retinal proteins, 255-258.
Hauser, F. E., Van Hazel, I. and Chang, B. S. W. (2014). Spectral tuning in vertebrate short wavelength-sensitive 1 (SWS1) visual pigments: Can wavelength sensitivity be inferred from sequence data? *J. Exp. Zool. Part B Mol. Dev. Evol.* **322**, 529-539. doi:10.1002/jez.b.22576
Hirayama, J., Imamoto, Y., Shichida, Y., Yoshizawa, T., Asato, A. E., Liu, R. S. H. and Kamo, N. (1994). Shape of the chromophore binding site in pharaonis phoborhodopsin from a study using retinal analogs. *Photochem. Photobiol.* **60**, 388-393. doi:10.1111/j.1751-1097.1994.tb05121.x
Hope, A. J., Partridge, J. C., Dulai, K. S. and Hunt, D. M. (1997). Mechanisms of wavelength tuning in the rod opsins of deep-sea fishes. *Proc. R. Soc. B Biol. Sci.* **264**, 155-163. doi:10.1098/rspb.1997.0023
Hunt, D. M., Carvalho, L. S., Cowing, J. A., Parry, J. W. L., Wilkie, S. E., Davies, W. L. and Bowmaker, J. K. (2007). Spectral tuning of shortwave-sensitive visual pigments in vertebrates. *Photochem. Photobiol.* **83**, 303-310. doi:10.1562/2006-06-27-IR-952
Hunt, D. M., Carvalho, L. S., Cowing, J. A. and Davies, W. L. (2009). Evolution and spectral tuning of visual pigments in birds and mammals. *Philos. Trans. R. Soc. B Biol. Sci.* **364**, 2941-2955. doi:10.1098/rstb.2009.0044
Irving, C. S., Byers, G. W. and Leermakers, P. A. (1970). Spectroscopic model for the visual pigments. influence of microenvironmental polarizability. *Biochemistry* **9**, 858-864. doi:10.1021/bi00806a020
Jiang, M., Pandey, S. and Fong, H. K. W. (1993). An opsin homologue in the retina and pigment epithelium. *Investig. Ophthalmol. Vis. Sci.* **34**, 3669-3678.
Katoh, K. and Standley, D. M. (2013). MAFFT multiple sequence alignment software version 7: improvements in performance and usability. *Mol. Biol. Evol.* **30**, 772-780. doi:10.1093/molbev/mst010
Kingston, A. C. N., Kuzirian, A. M., Hanlon, R. T. and Cronin, T. W. (2015). Visual phototransduction components in cephalopod chromatophores suggest dermal photoreception. *J. Exp. Biol.* **218**, 1596-1602. doi:10.1242/jeb.117945
Liénard, M. A., Bernard, G. D., Allen, A., Lassance, J.-M., Song, S., Childers, R. R., Yu, N., Ye, D., Stephenson, A., Valencia-Montoya, W. A. et al. (2021). The evolution of red color vision is linked to coordinated rhodopsin tuning in lycaenid butterflies. *Proc. Natl. Acad. Sci. USA* **118**, 1-12. doi:10.1073/pnas.2008986118
Lin, S. W., Kochendoerfer, G. G., Carroll, K. S., Wang, D., Mathies, R. A. and Sakmar, T. P. (1998). Mechanisms of spectral tuning in blue cone visual pigments: visible and Raman spectroscopy of blue-shifted rhodopsin mutants. *J. Biol. Chem.* **273**, 24583-24591. doi:10.1074/jbc.273.38.24583
Lythgoe, J. N., Baumann, C., Bridges, C. D. B., Crescitelli, F., Dartnall, H. J. A., Eakin, R. M., Falk, G., Fatt, P., Goldsmith, T. H., Hara, R. et al. (1972). The adaptation of visual pigments to the photic environment. *Photochem. Vis.* **7/1**, 566-603. doi:10.1007/978-3-642-65066-6_14
Macias-Muñoz, A., Rangel Olguin, A. G. and Briscoe, A. D. (2019). Evolution of Phototransduction Genes in Lepidoptera. *Genome Biol. Evol.* **11**, 2107-2124. doi:10.1093/gbe/evz150
Melaccio, F., Ferré, N. and Olivucci, M. (2012). Quantum chemical modeling of rhodopsin mutants displaying switchable colors. *Phys. Chem. Chem. Phys.* **14**, 12485-12495. doi:10.1039/c2cp40940b
Merbs, S. L. and Nathans, J. (1993). Role of hydroxyl-bearing amino acids in differentially tuning the absorption spectra of the human red and green cone pigments. *Photochem. Photobiol.* **58**, 706-710. doi:10.1111/j.1751-1097.1993.tb04956.x
Morrow, J. M. and Chang, B. S. W. (2010). The p1D4-hrGFP II expression vector: a tool for expressing and purifying visual pigments and other G protein-coupled receptors. *Plasmid* **64**, 162-169. doi:10.1016/j.plasmid.2010.07.002
Murakami, M. and Kouyama, T. (2008). Crystal structure of squid rhodopsin. *Nature* **453**, 363-367. doi:10.1038/nature06925
Nagata, T., Koyanagi, M., Tsukamoto, H., Mutt, E., Schertler, G. F. X., Deupi, X. and Terakita, A. (2019). The counterion–retinylidene Schiff base interaction of an invertebrate rhodopsin rearranges upon light activation. *Commun. Biol.* **2**, 1-9. doi:10.1038/s42003-019-0409-3
Nakayama, T. A. and Khorana, H. G. (1991). Mapping of the amino acids in membrane-embedded helices that interact with the retinal chromophore in bovine rhodopsin. *J. Biol. Chem.* **266**, 4269-4275. doi:10.1016/S0021-9258(20)64317-4
Nathans, J. (1990). Determinants of visual pigment absorbance: identification of the Retinylidene Schiff's Base Counterion in Bovine Rhodopsin. *Biochemistry* **29**, 9746-9752. doi:10.1021/bi00493a034
Neitz, M., Neitz, J. and Jacobs, G. H. (1991). Spectral tuning of pigments underlying red-green color vision. *Science (80-)* **252**, 971-974. doi:10.1126/science.1903559
Neitz, M., Neitz, J. and Jacobs, G. H. (2016). *Spectral Tuning of Pigments Underlying Red-Green Color Vision Author (s): Maureen Neitz, Jay Neitz and Gerald H*. Jacobs Published by: American Association for the Advancement of Science Stable. http://www.jstor.org/stable/2875359. Accessed: 07-0. 252: 971–974.
Oprian, D. D., Molday, R. S., Kaufman, R. J. and Khorana, H. G. (1987). Expression of a synthetic bovine rhodopsin gene in monkey kidney cells. *Proc. Natl. Acad. Sci. USA* **84**, 8874-8878. doi:10.1073/pnas.84.24.8874
Oprian, D. D., Pelletier, S. L., Asenjo, A. B. and Lee, N. (1991). Design, chemical synthesis, and expression of genes for the three human color vision pigments. *Biochemistry* **30**, 11367-11372. doi:10.1021/bi00112a002
Ozaki, K., Hara, R., Hara, T. and Kakitani, T. (1983). Squid retinochrome. Configurational changes of the retinal chromophore. *Biophys. J.* **44**, 127-137. doi:10.1016/S0006-3495(83)84285-4
Ozaki, K., Terakita, A., Hara, R. and Hara, T. (1986). Rhodopsin and retinochrome in the retina of a marine gastropod, Conomulex luhuanus. *Vision Res.* **26**, 691-705. doi:10.1016/0042-6989(86)90083-0
Pettersen, E. F., Goddard, T. D., Huang, C. C., Couch, G. S., Greenblatt, D. M., Meng, E. C. and Ferrin, T. E. (2004). UCSF Chimera - a visualization system for exploratory research and analysis. *J. Comput. Chem.* **25**, 1605-1612. doi:10.1002/jcc.20084
Ramirez, M. D., Pairett, A. N., Pankey, M. S., Serb, J. M., Speiser, D. I., Swafford, A. J. and Oakley, T. H. (2016). The last common ancestor of most bilaterian animals possessed at least nine opsins. *Genome Biol. Evol.* **8**, 3640-3652. doi:10.1093/gbe/evw248
Rinaldi, S., Melaccio, F., Gozem, S., Fanelli, F. and Olivucci, M. (2014). Comparison of the isomerization mechanisms of human melanopsin and

invertebrate and vertebrate rhodopsins. *Proc. Natl. Acad. Sci. USA* **111**, 1714-1719. doi:10.1073/pnas.1309508111

Saito, T., Koyanagi, M., Sugihara, T., Nagata, T., Arikawa, K. and Terakita, A. (2019). Spectral tuning mediated by helix III in butterfly long wavelength-sensitive visual opsins revealed by heterologous action spectroscopy. *Zool Lett.* **5**, 1-11. doi:10.1186/s40851-019-0150-2

Sekharan, S., Katayama, K., Kandori, H. and Morokuma, K. (2012). Color vision: "OH-site" rule for seeing red and green. *J. Am. Chem. Soc.* **134**, 10706-10712. doi:10.1021/ja304820p

Serb, J. M., Faggionato, D., Smedley, G. D., Seetharam, A., Severin, A. J. and Pairett, A. N. (2021). Expression and spectral analysis of twelve opsins reveals astonishing photochemical diversity in the common bay scallop Argopecten irradians (Mollusca: Bivalvia). *bioRix* doi.10.1101/2021.05.26.445805

Shichida, Y. and Matsuyama, T. (2009). Evolution of opsins and phototransduction. *Philos. Trans. R. Soc. Lond. B Biol. Sci.* **364**, 2881-2895. doi:10.1098/rstb.2009.0051

Shimamura, T., Hiraki, K., Takahashi, N., Hori, T., Ago, H., Masuda, K., Takio, K., Ishiguro, M. and Miyano, M. (2008). Crystal structure of squid rhodopsin with intracellularly extended cytoplasmic region. *J. Biol. Chem.* **283**, 17753-17756. doi:10.1074/jbc.C800040200

Shimono, K., Ikeura, Y., Sudo, Y., Iwamoto, M. and Kamo, N. (2001). Environment around the chromophore in pharaonis phoborhodopsin: mutation analysis of the retinal binding site. *Biochim. Biophys. Acta Biomembr.* **1515**, 92-100. doi:10.1016/S0005-2736(01)00394-7

Sperling, L. and Hubbard, R. (1975). Squid retinochrome. *J. Gen. Physiol.* **65**, 235-251. doi:10.1085/jgp.65.2.235

Surridge, A. K., Osorio, D. and Mundy, N. I. (2003). Evolution and selection of trichromatic vision in primates. *Trends Ecol. Evol.* **18**, 198-205. doi:10.1016/S0169-5347(03)00012-0

Terakita, A., Yamashita, T. and Shichida, Y. (2000). Highly conserved glutamic acid in the extracellular IV-V loop in rhodopsins acts as the counterion in retinochrome, a member of the rhodopsin family. *Proc. Natl. Acad. Sci. USA* **97**, 14263-14267. doi:10.1073/pnas.260349597

Terakita, A., Koyanagi, M., Tsukamoto, H., Yamashita, T., Miyata, T. and Shichida, Y. (2004). Counterion displacement in the molecular evolution of the rhodopsin family. *Nat. Struct. Mol. Biol.* **11**, 284-289. doi:10.1038/nsmb731

Terakita, A., Tsukamoto, H., Koyanagi, M., Sugahara, M., Yamashita, T. and Shichida, Y. (2008). Expression and comparative characterization of Gq-coupled invertebrate visual pigments and melanopsin. *J. Neurochem.* **105**, 883-890. doi:10.1111/j.1471-4159.2007.05184.x

Ueyama, H., Kuwayama, S., Imai, H., Tanabe, S., Oda, S., Nishida, Y., Wada, A., Shichida, Y. and Yamade, S. (2002). Novel missense mutations in red/green opsin genes in congenital color-vision deficiencies. *Biochem. Biophys. Res. Commun.* **294**, 205-209. doi:10.1016/S0006-291X(02)00458-8

Van Hazel, I., Sabouhanian, A., Day, L., Endler, J. A. and Chang, B. S. W. (2013). Functional characterization of spectral tuning mechanisms in the great bowerbird short-wavelength sensitive visual pigment (SWS1), and the origins of UV/violet vision in passerines and parrots. *BMC Evol. Biol.* **13**, 250. doi:10.1186/1471-2148-13-250

Varma, N., Mutt, E., Mühle, J., Panneels, V., Terakita, A., Deupi, X., Nogly, P., Schertler, G. F. X. and Lesca, E. (2019). Crystal structure of jumping spider rhodopsin-1 as a light sensitive GPCR. *Proc. Natl. Acad. Sci. USA* **116**, 14547-14556. doi:10.1073/pnas.1902192116

Vöcking, O., Kourtesis, I., Tumu, S. C. and Hausen, H. (2017). Co-expression of xenopsin and rhabdomeric opsin in photoreceptors bearing microvilli and cilia. *eLife* **6**, e23435. doi:10.7554/eLife.23435

Wakakuwa, M., Terakita, A., Koyanagi, M., Stavenga, D. G., Shichida, Y. and Arikawa, K. (2010). Evolution and mechanism of spectral tuning of Blue-absorbing visual pigments in butterflies. *PLoS ONE* **5**, 1-8. doi:10.1371/journal.pone.0015015

Yang, J., Roy, A. and Zhang, Y. (2013a). BioLiP: a semi-manually curated database for biologically relevant ligand-protein interactions. *Nucleic Acids Res.* **41**, 1096-1103. doi:10.1093/nar/gks966

Yang, J., Roy, A. and Zhang, Y. (2013b). Protein-ligand binding site recognition using complementary binding-specific substructure comparison and sequence profile alignment. *Bioinformatics.* **29**, 2588-2595. doi:10.1093/bioinformatics/btt447

Yokoyama, S. (2000a). Molecular evolution of vertebrate visual pigments. *Prog. Retin. Eye Res.* **19**, 385-419. doi:10.1016/S1350-9462(00)00002-1

Yokoyama, S. (2000b). Phylogenetic analysis and experimental approaches to study color vision in vertebrates. *Methods Enzymol.* **315**, 312-325. doi:10.1016/s0076-6879(00)15851-3

Yokoyama, S. (2008). Evolution of dim-light and color vision pigments. *Annu. Rev. Genomics Hum. Genet.* **9**, 259-282. doi:10.1146/annurev.genom.9.081307.164228

Yokoyama, S. and Radlwimmer, F. B. (1998). The "five-sites" rule and the evolution of red and green color vision in mammals. *Mol. Biol. Evol.* **15**, 560-567. doi:10.1093/oxfordjournals.molbev.a025956

Yokoyama, S. and Radlwimmer, F. (1999). The molecular genetics of red and green color vision in mammals. *Genetics* **153**, 919-932. doi:10.1093/genetics/153.2.919

Yokoyama, S., Xing, J., Liu, Y., Faggionato, D., Altun, A. and Starmer, W. T. (2014). Epistatic Adaptive Evolution of Human Color Vision. *PLoS Genet.* **10**, e1004884. doi:10.1371/journal.pgen.1004884

Yokoyama, S., Altun, A., Jia, H., Yang, H., Koyama, T., Faggionato, D., Liu, Y. and Starmer, W. T. (2015). Adaptive evolutionary paths from UV reception to sensing violet light by epistatic interactions. *Sci. Adv.* **1**. doi:10.1126/sciadv.1500162

Zhang, J., Yang, J., Jang, R. and Zhang, Y. (2015). GPCR-I-TASSER: A Hybrid Approach to G Protein-Coupled Receptor Structure Modeling and the Application to the Human Genome. *Structure.* **23**, 1538-1549. doi:10.1016/j.str.2015.06.007

```
Bov-Rho_prot      1 MNGTEGPNFYVPFSNKTGVVRSPFEAPQYYLAEPWQFSMLAAYMFLLIML  50
Pmax-RTC_prot     1 ------------MSSPTDTAVGMFSA--------WEFRCVGIAYFIFGSA  30
Air-RTC_prot      1 ------------MSSPTDTAVGMFSV--------WEFRFVGIAYFVFGSA  30
Tpac-RTC_prot     1 ----------MFGNPAMTGLHQFTM--------WEHYFTGSIYLVLGCV  31

Bov-Rho_prot     51 GFPINFLTLYVTVQHKKLRTPLNYILLNLAVADLFMVFGGFTTTLYTSLH 100
Pmax-RTC_prot    31 GVLANAFTILTFMRESPISSPRHILQLNMAIANL-LVCAPFPFSGLSSFR  79
Air-RTC_prot     31 GVLANAFTILTFMRESPIGSPRHILQLNMAIANL-LVCAPFPFSGLSSFK  79
Tpac-RTC_prot    32 VFSLCGMCIIFLARQSPKPRRKYAILIHVLITAM-AVNGGDPAHASSSIV  80

Bov-Rho_prot    101 GYFVFGPTGCNLEGFFATLGGEIALWSLVVLAIERYVVVCKPMSNFRFGE 150
Pmax-RTC_prot    80 GKWLFGDLGCQLYGTESFLGGMAATTFIPVVCIEHYLVSCRKDFYDTISS 129
Air-RTC_prot     80 GQWLFGELGCQLYGTESFLGGMAATTFIPVVCIEHYLASCKKDFYDTISS 129
Tpac-RTC_prot    81 GRWLYGSVGCQLMGFWGFFGGMSHIWMLFAFAMERYMAVCHREFYQQMPS 130
                                                  †
Bov-Rho_prot    151 NHAIMGVAFTWVMALACAAPPLVGWSRYIPEGMQCSCGIDYYTPHEETNN 200
Pmax-RTC_prot   130 GTWWTVAMLCWMYASLWAILPLFGWNSYDVESSGIACGINWLR--KDSNH 177
Air-RTC_prot    130 STWWTVAMLCWMYAALWAILPLFGWNSYDVESSGIACGINWLK--KDASH 177
Tpac-RTC_prot   131 VYYSIIVGLMYTFGTFWATMPLLGWASYGLEVHGTSCTINYSV--SDESY 178

Bov-Rho_prot    201 ESFVIYMFVVHFIIPLIVIFFCYGQL---VFTVKEAAAQQQESATTQKAE 247
Pmax-RTC_prot   178 MTYLQAMVI-TWLILFAMAFYGLYQSRVYWESVQTKADPKPDT-KNWFTE 225
Air-RTC_prot    178 ITYMQAMVI-TYLILFVMAFYGLYQSRVYWESVQVKADPKPDA-KNWFTE 225
Tpac-RTC_prot   179 QSYVFFLAIFSFIFPMVSGWYAISKA---WSGLSAIPDAEKEKDKDILSE 225
                                                                  ‡
Bov-Rho_prot    248 KEVTRMVIIMVIAFLICWLPYAGVAFY-IFTHQGSDFGPIFMTIPAFFAK 296
Pmax-RTC_prot   226 RQQAWICLAFMGIMCVGFGPYAILGAWAALT-DSTTVSTLAIIIPSLACK 274
Air-RTC_prot    226 RQQAWICLAFMGIMCIGFGPYAILGAWSALT-DSTTVSTLAIIIPSLACK 274
Tpac-RTC_prot   226 EQLTALAGAFILISLISWSGFGYVAIYSALTHGGAQLSHLRGHVPPIMSK 275

Bov-Rho_prot    297 TSAVYNPVIYIMMNKQFRNCMVTTLCCGKNPLGDDEASTTVSKTETSQVA 346
Pmax-RTC_prot   275 ASSSLYPIPYIVASDRFRAAYL----------------GYRVSEQEAK--A 307
Air-RTC_prot    275 ASSSLYPLPYIVASDKFRAAYL----------------GYRVSEQEAK--A 307
Tpac-RTC_prot   276 TGCALFPLLIFLLTAR----------------------SLPKSDTK--K 300

Bov-Rho_prot    347 PA                                              348
Pmax-RTC_prot       --
Air-RTC_prot    308 N-                                              308
Tpac-RTC_prot   301 P-                                              301
```

Fig S1. Protein alignment of scallop (Air-RTC, Pmax-RTC) and squid (Tpac-RTC) retinochrome with bovine rhodopsin (Bov-Rho). Alignment follows numbering system of Bov-Rho. Glutamate (E) counterion and the retinal-binding Lysine (K) in blue, indicated by † and ‡, respectively. Mutation sites in this study and their homologous positions in bovine and squid are shown in three boxes.

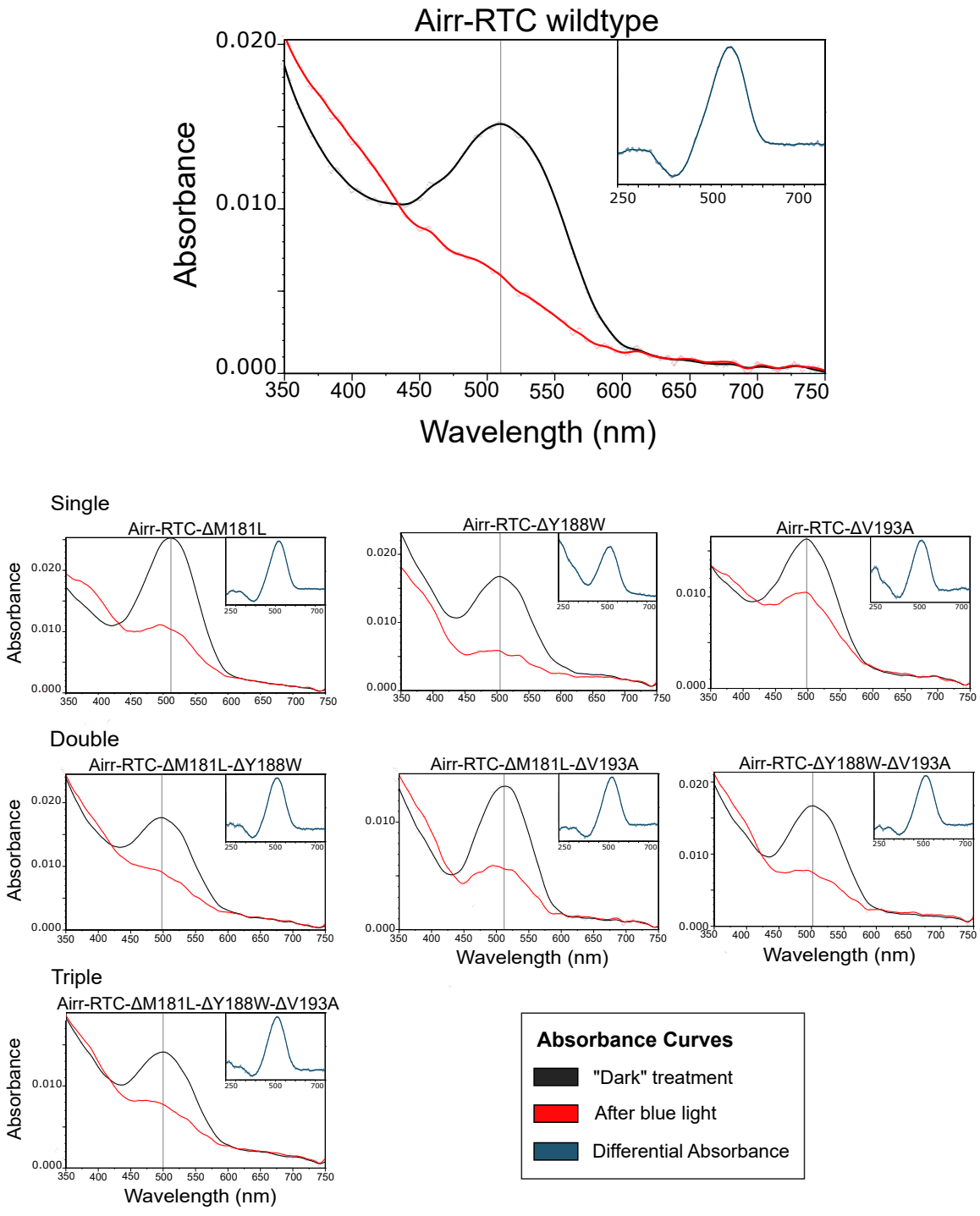

Fig S2. Unfitted spectral data of mutant *Argopecten irradians* retinochrome. Black curves plot of the average of five dark (unexposed) spectra and red curves show the average of five spectra after 3-minute exposure to blue light. Vertical black lines indicate maximum absorption peaks of unfitted data. Insets show the differential absorbance of the dark spectrum minus the spectrum recorded after irradiation with blue light.

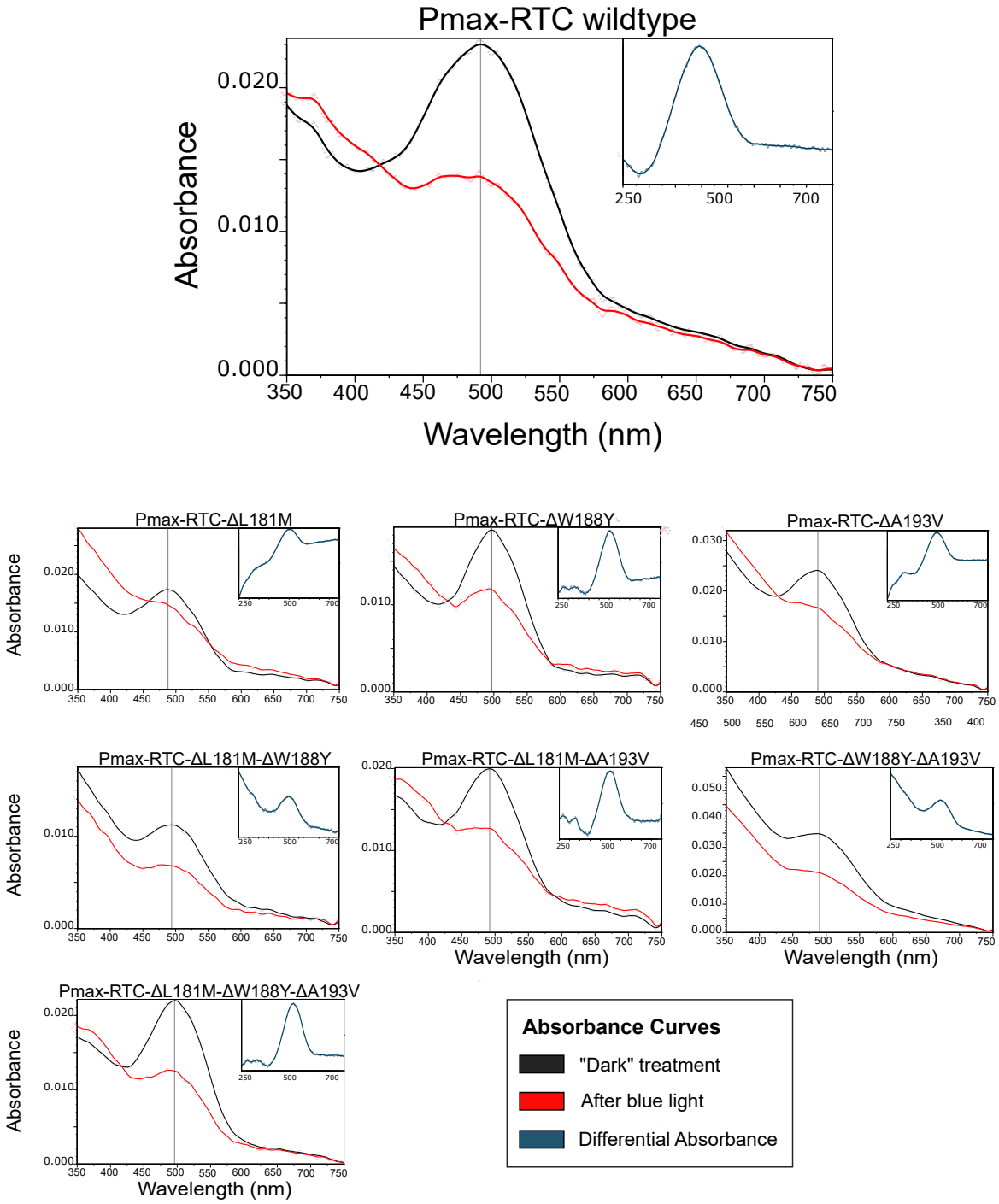

Fig S3. Unfitted spectral data of mutant *Pecten maximus* retinochrome. Black curves plot of the average of five dark (unexposed) spectra and red curves show the average of five spectra after 3-minute exposure to blue light. Vertical black lines indicate maximum absorption peaks of unfitted data. Insets show the differential absorbance of the dark spectrum minus the spectrum recorded after irradiation with blue light.

Table S1. Primer sequences and annealing temperatures used in cloning of wild-type retinochromes and the creation of the seven mutants.

Cloning Target	Sequence (5' to 3')	Annealing temp (°C)
Airr-RTC:		
Out-UTR_F	TGCATGGCAGTGGCTCGGAA	Step up 49 – 54°C
Out-UTR_R	ACGTCACTCGTTTCCTGTCTCAACA	Step up 49 – 54°C
In-UTR_F	CACATTTGATAGAATTGCTCTCG	Step up 49 – 54°C
In-UTR_R	CCTGACTGAAAATAGATAAATCTCTG	Step up 49 – 54°C
BamHI site	ATGCGGATCCCACCATGAGCTCCCCTACAGATACCG	55°C
EcoR1 site	GCATGAATTCTTGGCCTTGGCTTCCTGTTC	55°C
Pmax-RTC:		
Out-UTR_R	CCACGGACGCGGGGGTATTG	Step up 49 – 54°C
In-UTR_F	GCACAGTGTTAGATAGAGCTCGAGGG	Step up 49 – 54°C
In-UTR_R	TGCCTGGCGGAGGACCTTCA	Step up 49 – 54°C
BamHI site	GCGGATCCCACCATGTCGTCACCTACTGATAC	55°C
EcoR1 site	GCATGAATTCTTGGCCTTGGCTTCCTGC	55°C
Airr-RTC ΔM181L:		
Forward	GAGTCACATTACGTACCTGCAGGCGATGGTAATC	60°C
Reverse	TAATGGTAGCGGACGTCCATGCATTACACTGAGC	60°C
Airr-RTC ΔW188Y:		
Forward	AGGCGATGGTAATCACGTGGCTCATTCTCTTTGTCATGG	60°C
Reverse	GTACTGTTTCTCTTACTCGGTGCACTAATGGTAGCGGAC	60°C
Airr-RTC ΔV193A:		
Forward	GTACCTCATTCTCTTTGCCATGGCGTTTTACGGAC	60°C
Reverse	CAGGCATTTTGCGGTACCGTTTCTCTTACTCCATG	60°C
Airr-RTC ΔW188Y+V193A:		
Forward	CACGTGGCTCATTCTCTTTGCCATGGCGTTTTAC	60°C
Reverse	GTAAAACGCCATGGCAAAGAGAATGAGCCACGTG	60°C
Pmax-RTC ΔL181M:		
Forward	AACCACATGACCTACATGCAGGCAATGGTAATCACGT	60°C
Reverse	CGTGATTACCATTGCCTGCATGTAGGTCATGTGGTTC	60°C
Pmax-RTC ΔY188W:		
Forward	GCAGGCAATGGTAATCACGTACCTCATTCTCTTTGCC	60°C
Reverse	GCAAAGAGAATGAGGTACGTGATTACCATTGCCTGCA	60°C
Pmax-RTC ΔA193V:		
Forward	GTCCGTAGAAAGCCATGACAAAGAGAATGAGCCAC	60°C
Reverse	GTGGCTCATTCTCTTTGTCATGGCTTTCTACGGAC	60°C
Pmax-RTC ΔY188W+A193V:		
Forward	CACGTACCTCATTCTCTTTGTCATGGCTTTCTACGGACT	60°C
Reverse	GTCCGTAGAAAGCCATGACAAAGAGAATGAGGTACGTGA	60°C